Trench-Isolated Low Gain Avalanche Diodes (TI-LGADs)

G. Paternoster*, *Member, IEEE*, G. Borghi*, *Member, IEEE*, M. Boscardin, N. Cartiglia, M. Ferrero, F. Ficorella, F. Siviero, A.Gola, P. Bellutti

***Abstract*— We present a novel design of fine segmented low gain avalanche diodes (LGAD) based on trench-isolation technique. The proposed design reduces the width of the no-gain inter-pad region down to less than 10 μm, from the 20-80 μm of the current LGAD technology, enabling the production of sensors with small pixel pitch and high fill-factor. Prototypes of this new technology were produced in the FBK laboratories. Their electrical characterization in terms of I-V, gain measurement and response to a focused laser, indicates that the trenches provide electrical isolation among pixels without any increase in the dark current level and without affecting the gain of the sensor. In addition, I-V measurements of p-i-n diodes with the same trench-isolation structure demonstrate that such termination scheme can withstand more than 500 Volts without reaching breakdown. This is well above the typical operating bias voltage of LGADs, thus confirming that trench-isolation is a promising solution for finely pixelated LGAD sensors.**

***Index Terms*— Deep Trench Isolation, LGAD, pixel segmentation, Trench.**

I. Introduction

LOW gain avalanche diodes (LGADs) are silicon sensors characterized by an internal charge-multiplying structure that provides low gain (a factor $\mathcal{O}(10)$) [1]. These devices are considered the enabling technology for 4-D tracking applications in high energy physics (HEP) experiments [2], [3] thanks to their outstanding timing resolution ($\sigma_t \sim 30$ ps for minimum ionizing particles) after being exposed to fluences up to about 10^{15} neq/cm^2 [4], [5]. Nevertheless, 4-D tracking applications are still limited by the relatively coarse segmentation that can be obtained with the current LGAD technologies, in the range $50\,\mu\text{m}$ – $1\,\text{mm}$. Indeed, the presence of isolation structures between adjacent pixels introduces a no-gain region where the signal is not multiplied, thus reducing the fill factor (FF) of small pixels to values below 0.5 (FF = pixel area with signal multiplication / total pixel area).

Submitted December 6, 2019; date of current version March, 28, 2019.

* G. Borghi and G. Paternoster equally contributed to this paper. Corresponding author: G. Paternoster (e-mail: paternoster@fbk.eu).

G. Paternoster, G. Borghi, M. Boscardin, F. Ficorella, A. Gola and P. Bellutti are with Fondazione Bruno Kessler, Via Sommarive 18, 38123 Trento, Italy, and TIFPA-INFN, Via Sommarive 18, 38123 Trento, Italy.

N. Cartiglia, M. Ferrero and F. Siviero are with Istituto Nazionale di Fisica Nucleare, Sezione di Torino and Università degli Studi di Torino, Via P. Giuria 1, 10125 Torino, Italy.

Recently, two new segmentation strategies have been proposed to overcome this limitation: i) inverse LGADs (i-LGADs) [6], [7]; ii) Resistive silicon detectors (RSDs), also known as AC-coupled LGADs (AC-LGADs) [8]. Both technologies are based on unsegmented multiplication junctions to avoid the FF losses due to the junction segmentation. In i-LGADs, the segmentation is transferred to the p^{++} ohmic back-side of the sensor. i-LGADs therefore require a full double-side photolithographic technology, for which thick, fully-depleted float-zone substrates (at least $275\,\mu\text{m}$) have to be used. In this design, the active volume is thicker than in standard LGADs, which are usually produced on thinner active substrates (about $50\,\mu\text{m}$) grown on or attached to thick support wafers. A thicker active volume leads to worse time resolution as discussed in [9]. The RSD technology, instead, maintains the same single side architecture of standard LGADs. It features single n+ resistive large contact and the fine segmentation readout is obtained via AC metal pads, capacitively coupled via a thin dielectric film. In these sensors, the signal on the AC pad is induced after the multiplied electrons are collected in the resistive n+ layer, when the signal discharges to ground. This mechanism of signal formation might have drawbacks in high-count-rate environments: the resistive layer might not drain the charge fast enough, determining baseline shifts, or multiple hits could determine excessive cross talk.

An alternative solution for LGAD segmentation is the deep trench isolation (DTI) technology, which exploits physical trenches in the silicon substrate to provide electrical isolation among nearby pixels. Such a solution has been extensively used in CMOS image sensors [10] as well as in silicon photomultipliers [11], where DTI reduces both electrical and optical cross-talk among cells [12].

In this paper, we present the application of DTI technology to LGAD design: trench-isolated LGADs (TI-LGADs) are designed to attain fine pixel segmentation and very high FF, preserving the timing capabilities and the radiation hardness of standard LGADs (STD-LGADs). Prototypes of this new technology were produced in the FBK laboratories; preliminary electrical characterization is reported and discussed in this paper.

II. Design and Simulations of Trench-Isolated LGAD

Fig. 1 reports not-to-scale cross sectional view of an LGAD (a) with standard segmentation and (b) with the novel proposed trench-isolated design. Both detectors are based on the

same $n^+/p^+/p^-/p^{++}$ junction scheme, where the extra p^+ region (or gain implant) defines the multiplication region, which produces carrier multiplication by means of the "impact ionization" effect. More details on the technology of the multiplication junction used in this work are reported in [13].

In standard LGADs, neighboring pixels are electrically isolated by means of a narrow p^+ ring (p-stop), which separates the n^+ regions of the pixels. In addition, to prevent premature breakdown (BD) at the pixel borders, a virtual guard ring (vGR) and a junction termination extension (JTE) are implemented at the pixel edge [14]. In particular, vGR consists of a gap between the end of the gain implant and the n^+ edges, while JTE is a deep low-concentration n-type region at the junction edge. These termination structures use some of the sensor's area and, as a consequence, introduce an inter-pixel region in which the gain is completely suppressed. This is the so-called no-gain region, defined as the distance between two adjacent gain implant regions. In standard FBK-LGAD productions, the no-gain region typically ranges in $31-66\,\mu m$, depending on the fabrication technology and device design, even if sensor prototypes with $20.5\,\mu m$ no-gain region width have been recently produced and preliminarily tested.

In the TI-LGADs design, the multiplying core structure is preserved but the standard pixel termination structures are completely replaced with a deep and narrow trench (less than $1\,\mu m$ wide and a few microns deep), which is filled with silicon dioxide. The trench acts as a physical barrier for electron drift/diffusion and provides electrical isolation among pixels. However, the presence of a Si/SiO_2 trench interface can lead to two possible issues: i) the formation of a conductive path due to fixed oxide charge density in SiO_2, shorting the pixels; ii) a significant surface generation at the highly-defective Si/SiO_2 interface and thus to a higher leakage current. The DTI structure developed by FBK solves these problems by using a proprietary design at the pixel border and in the trench regions. This design makes possible to obtain a complete pixel electrical isolation and to prevent any detector noise increase due to DTI. In particular, regarding the latter point, the borders of the multiplication region have been suitably engineered (the details of the junction design are not represented in the figure) with the aim to drift the carriers generated at the trench interface outside the multiplication region. The novel scheme allows to reduce the nominal no-gain region down to $\sim 5\,\mu m$, which is a factor of 5 lower with respect to the state-of-the-art STD-LGAD design.

Numerical simulations (SILVACO simulation tools [15]) have been used to investigate the gain variation at the border region both in the standard LGADs and in TI-LGADs. The simulated structure were defined analytically using SILVACO DEVEDIT tool. The doping profiles were obtained either using SIMS measurements or simulating 1D implant profiles with SILVACO ATHENA tool. TCAD device simulations were performed using SILVACO ATLAS tool. The simulation model was calibrated using experimental data obtained with standard LGADs, such as the results presented in [16]. The simulated STD-LGAD and TI-LGAD have nominal no-gain region widths of $20.5\,\mu m$ (the minimum value available at FBK with standard technology) and $\sim 4\,\mu m$, respectively.

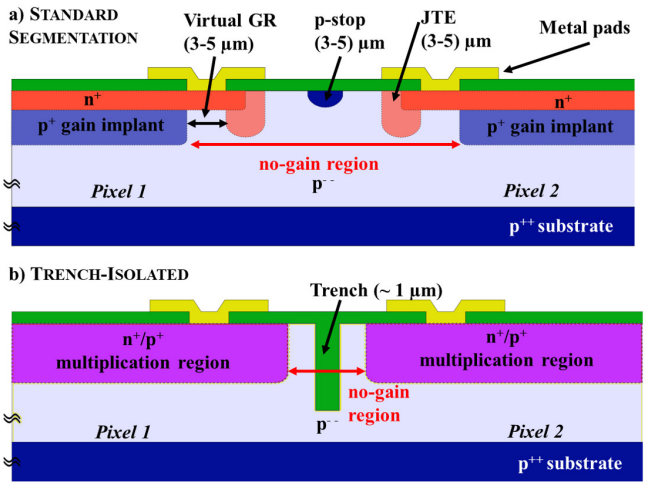

Fig. 1. Schematic drawings of a standard LGAD (a) and of the proposed trench-isolated LGAD (b).

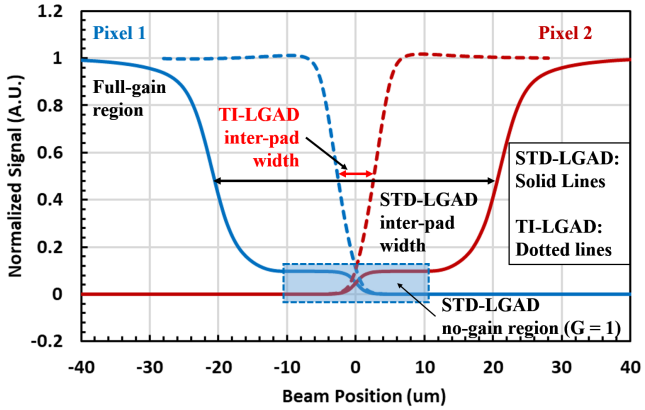

Fig. 2. TCAD simulations of a laser scan through the border region of two LGAD pixels for both standard (solid lines) and trench-isolated (dotted lines) LGADs.

A scan through the border region between two pixels with a 1-µm-wide uniform IR laser beam ($1064\,nm$) has been simulated for both structures. The scan was performed using static (DC) conditions, since preliminary tests showed that transient and static simulations provide the same results and static simulations require less computational resources. Fig. 2 presents the normalized intensity of the simulated signal generated in each pixel by the laser as a function of its position (i.e. the current measured on the pixel with the beam on minus the current measured on the pixel with the beam off). With reference to Fig. 2, the effective inter-pad width can be defined as the distance between two adjacent pixels where the signal is less than 50% of the signal at the pixel core. In standard LGADs, the simulated inter-pad width is $41 \pm 1\,\mu m$, while in the TI-LGAD it is reduced to only $5.5 \pm 0.5\,\mu m$. It is interesting to stress that the effective inter-pad width ($41\,\mu m$) and the nominal no-gain value ($20.5\,\mu m$) are quite different in the standard LGAD design, while the values are similar in the TI-LGAD design. TCAD simulations suggest that this effect is due to the presence of JTE and vGR that perturb the electric field at the pixel border. In standard LGADs, carriers

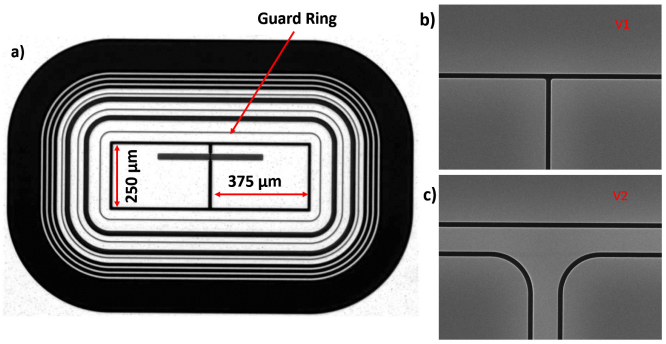

Fig. 3. Picture of a TI-LGAD at the end of the fabrication process (a). SEM images of trench before filling process are reported and they refer to the V1 (b) and V2 (c) layout version, respectively.

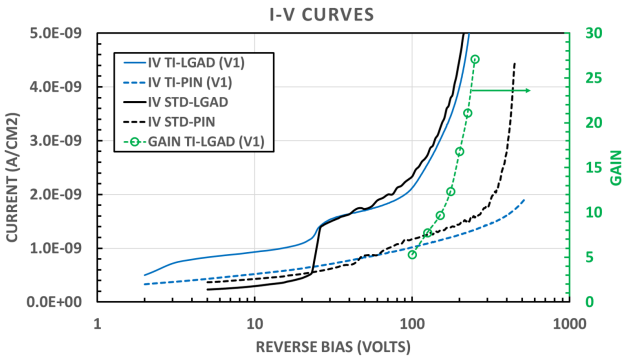

Fig. 4. I-V curves of: TI-LGAD (V1) (blue solid line) and respective p-i-n (blue dotted line); Standard LGAD (black solid line) and p-i-n (black dotted line). The gain of the TI-LGAD is also reported in green.

generated at the periphery of the gain implant region are partially or totally collected by the deeper JTE implant instead of drifting through the multiplication region, thus increasing the effective gain-loss region. It is worth noting that the not-multiplied charges collected at the JTE region generate signals with $G = 1$ (plateau highlighted in blue in Fig. 2), thus leading to a degradation of the spectral performance of the detector. On the other side, TI-LGADs do not exhibits any plateau corresponding to signals with unitary gain.

A TCAD simulation campaign was also set up in order to optimize the TI-LGAD design in terms of trench geometry, i.e. shape, width and depth. The most promising structures have been identified and implemented in a detector production.

III. Device Production and Characterization

Prototypes of TI-LGADs have been produced at FBK laboratories (Trento, Italy) based on a custom CMOS-like fabrication technology. The sensors have been fabricated on p^-/p^{++} wafers with a $55\,\mu m$ thick epitaxial layer, using the same multiplication junction technology (ion implantation dose and energy of the doped regions, thermal annealing) used in standard LGAD productions at FBK [13]. The trenches have been etched after the junction formation by means of deep reactive ion etching (DRIE) technique, which allows creating trenches with a high aspect ratio. The trenches are less than $1\,\mu m$ wide and deeper than the gain-implant depth. After the etching, the trenches have been oxidized and filled by means of CVD-deposited silicon dioxide. A picture of the detector at the end of the fabrication process is reported in Fig. 3a. To facilitate the electrical characterization, the detector layout consists in two pixels ($250\,\mu m \times 375\,\mu m$) enclosed by a common guard ring structure, obtained with a set of 1 biased and 5 floating n^{++} rings around the sensor (the same structure used in standard FBK-LGADs). Many layout splits, with different trench geometries, have been produced; among the others: *V1* split features a simple trench grid to isolate the pixels (fig. 3b); in *V2* split, each pixel is surrounded by a trench ring and thus two trenches are present between adjacent pixels (fig. 3c). In version *V1*, the nominal no-gain region width is ~ 4 µm, whereas in version *V2* it is ~ 6 µm.

In fig. 4 the IV curve of a TI-LGAD sensor (version *V1*, which corresponds to the structure used in the simulations) measured at room temperature under dark conditions is reported (blue solid line) together with a reference p-i-n diode with the same trench-isolation layout (blue dotted line) but without the gain layer. The IV curves of a standard LGAD (produced in the same batch using the same multiplication junction technology) and of the respective p-i-n diode are also plotted with black solid and dotted lines, respectively, for a direct comparison. It is worth noting that both TI-LGAD and standard LGAD feature the characteristic "knee" at about $25\,V$, which indicates the full depletion of the gain layer. At higher voltages, the leakage current of both the LGAD samples increases due to the increasing internal gain and then reaches the breakdown at about $300\,V$, due to gain divergence. This is confirmed by the behavior of the gain (green open circles), which has been measured on the TI-LGAD by using a $1064\,nm$ laser setup and a broad-band amplifier [13]. The gain has been calculated as the charge of the LGAD with respect to that of the reference p-i-n diode. The same setup has been also used to acquire simultaneously the signals from both the pixels, thus demonstrating the complete electrical isolation between the pads.

In the p-i-n diodes, due to the absence of gain, the current remains almost constant up to breakdown (most likely at the pixel border). This breakdown happens at about $350\,V$ for the standard p-i-n, while no breakdown occurs up to $500\,V$ for the trench-isolated p-i-n, indicating a good behavior of the trench isolation border.

IV. Conclusions

A novel LGAD design based on trench-isolated technology has been presented, and prototypes of this new technology have been successfully produced at FBK. Preliminary measurements showed proper isolation between pixels, high breakdown voltage at the pixel border and gain values in the range $5 - 25$. Numerical simulations also showed that TI-LGADs can reduce the width of the gain-loss region down to ~ 6 µm. Both these characteristics pave the way for the realization of segmented LGADs with pixel pitch down to $50\,\mu m$ and FF higher than 75%.

REFERENCES

[1] G. Pellegrini, P. Fernandez-Martınez, M. Baselga, C. Fleta, D. Flores, V. Greco, S. Hidalgo, I. Mandiè, G. Kramberger, D. Quirion, M. Ullan, "Technology developments and first measurements of Low Gain Avalanche Detectors (LGAD) for high energy physics applications", Nucl. Instrum. Methods Phys. Res. A, vol. 765, pp. 12–16, 2014, DOI: 10.1016/j.nima.2014.06.008.

[2] N. Cartiglia, R. Arcidiacono, B. Baldassarri, M. Boscardin and F. Cenna, G. Dellacasa, G.-F. Dalla Betta, M. Ferrero, V. Fadeyev, Z. Galloway, S. Garbolino, H. Grabas, V. Monaco, M. Obertino, L. Pancheri, G. Paternoster, A. Rivetti, M. Rolo, R. Sacchi, H. Sadrozinski, A. Seiden, V. Sola, A. Solano, A. Staiano, F. Ravera, A. Zatserklyaniy, "Tracking in 4 dimensions", Nucl. Instrum. Methods Phys. Res. A, vol. 845, pp. 47–51, 2017, DOI: 10.1016/j.nima.2016.05.078.

[3] H. F.-W. Sadrozinski, A. Seiden, N. Cartiglia, "4D tracking with ultra-fast silicon detectors", Reports on Progress in Physics 81 (2), 2018, DOI: 10.1088/1361-6633/aa94d3.

[4] M. Carulla, A. Doblas, D. Flores, Z. Galloway, S. Hidalgo, G. Kramberger, Z. Luce, I. Mandic, S. Mazza, A. Merlos, G. Pellegrini, D. Quirion, R. Rodríguez, H.F.-W. Sadrozinski, A. Seiden, Y. Zhao, "50 μm thin Low Gain Avalanche Detectors (LGAD) for timing applications", Nucl. Instrum. Methods Phys. Res. A, vol. 924, no. August, pp. 373–379, 2019, DOI: 10.1016/j.nima.2018.08.041

[5] V. Sola, R. Arcidiacono, M. Boscardin, N. Cartiglia, G. F. Dalla Betta, F. Ficorella, M. Ferrero, M. Mandurrino, L. Pancheri, G. Paternoster, A. Staiano, "First FBK production of 50 μm ultra-fast silicon detectors", Nucl. Instruments Methods Phys. Res. Sect. A Accel. Spectrometers, Detect. Assoc. Equip., vol. 924, no. July, pp. 360–368, 2019, DOI: 10.1016/j.nima.2018.07.060.

[6] F. F. Dalla Betta, L. Pancheri, M. Boscardin, G. Paternoster, C. Piemonte, N. Cartiglia, F. Cenna, M. Bruzzi, "Design and TCAD simulation of double-sided pixelated low gain avalanche detectors", Nucl. Instruments Methods Phys. Res. Sect. A Accel. Spectrometers, Detect. Assoc. Equip., vol. 796, pp. 154-157, 2015, DOI: 10.1016/j.nima.2015.03.039.

[7] G. Pellegrini, M. Baselga, M. Carulla, V. Fadeyev, P. Fernández-Martínez, M. Fernández García, D. Flores, Z. Galloway, C. Gallrapp, S. Hidalgo, Z. Liang, A. Merlos, M. Moll, D. Quirion, H. Sadrozinski, M. Stricker, I. Vila, "Recent technological developments on LGAD and iLGAD detectors for tracking and timing applications", Nucl. Instruments Methods Phys. Res. Sect. A, vol. 831, pp. 24–28, 2016, DOI: 10.1016/j.nima.2016.05.066.

[8] M. Mandurrino, R. Arcidiacono, M. Boscardin, N. Cartiglia, G. F. Dalla Betta, M. Ferrero, F. Ficorella, L. Pancheri, G. Paternoster, F. Siviero, M. Tornago, "Demonstration of 200, 100, and 50 μm pitch Resistive AC-Coupled Silicon Detectors (RSD) with 100% fill-factor for 4D particle tracking", in IEEE Electron Device Letters, vol. 40, no. 11, pp. 1780-1783, Nov. 2019, DOI: 10.1109/LED.2019.2943242.

[9] N. Cartiglia, R. Arcidiacono, M. Baselga, R. Bellan, M. Boscardin, F. Cenna, G.F. Dalla Betta, P. Fernndez-Martnez, M. Ferrero, D. Flores, Z. Galloway, V. Greco, S. Hidalgo, F. Marchetto, V. Monaco, M. Obertino, L. Pancheri, G. Paternoster, A. Picerno, G. Pellegrini, D. Quirion, F. Ravera, R. Sacchi, H.F.-W. Sadrozinski, A. Seiden, A. Solano, N. Spencer, "Design optimization of ultra-fast silicon detectors", Nucl. Instruments Methods Phys. Res. Sect. A Accel. Spectrometers, Detect. Assoc. Equip., vol. 796, pp. 141-148, 2015, DOI: doi.org/10.1016/j.nima.2015.04.025.

[10] Tournier, A., F. Leverd, L. Favennec, C. Perrot, L. Pinzelli, M. Gatefait, N. Cherault, D. Jeanjean, J.-P. Carrere, F. Hirigoyen, L. Grant, F. Roy, Application to CMOS image sensor", Proceedings of Internatinal Image Sensor Workshop, 2011.

[11] C. Piemonte, F. Acerbi, A. Ferri, A. Gola, G. Paternoster, V. Regazzoni, G. Zappala, N. Zorzi, "Performance of NUV-HD Silicon Photomultiplier Technology", in IEEE Transactions on Electron Devices, vol. 63, no. 3, pp. 1111-1116, March 2016, DOI: 10.1109/TED.2016.2516641

[12] Ch. Dietzinger, P. Iskra, Thomas Ganka, T. Eggert, Lothar Höllt, A. Pahlke, N. Miyakawa, M. Fraczek, J. Knobloch, F. Wiest, W. Hansch, R. Fojt, "Reduction of optical crosstalk in silicon photomultipliers", Biosensing and Nanomedicine V. Vol. 8460. International Society for Optics and Photonics, 2012, DOI: doi.org/10.1117/12.930473

[13] G. Paternoster, R. Arcidiacono, M. Boscardin, N. Cartiglia, F. Cenna, G.F. Dalla Betta, M. Ferrero, R. Mulargia, M. Obertino, L. Pancheri, C. Piemonte, V. Sola "Developments and first measurements of Ultra-Fast Silicon Detectors produced at FBK", Journal of Instrumentation 12.02, 2017, DOI: 10.1088/1748-0221/12/02/C02077

[14] P. Fernández-Martínez, D. Flores, S. Hidalgo, V. Greco, A. Merlos, G. Pellegrini, D. Quirion, "Design and Fabrication of an Optimum Peripheral Region for Low Gain Avalanche Detectors", Nucl. Instrum. Methods Phys. Res. A 821, pp. 93–100, 2016, DOI: 10.1016/j.nima.2016.03.049.

[15] SILVACO TCAD simulation tools, https://www.silvaco.com/

[16] M. Andrä, J. Zhang, A. Bergamaschi, R. Barten, C. Borca, G. Borghi, M. Boscardin, P. Busca, M. Brückner, N. Cartiglia, S. Chiriotti, G. F. Dalla Betta, R. Dinapoli, P. Fajardo, M. Ferrero, F. Ficorella, E. Fröjdh, D. Greiffenberg, T. Huthwelker, C. Lopez-Cuenca, M. Meyer, D. Mezza, A. Mozzanica, L. Pancheri, G. Paternoster, S. Redford, M. Ruat, C. Ruder, B. Schmitt, X. Shi, V. Sola, D. Thattil, G. Tinti, S. Vetter, "Development of low-energy X-ray detectors using LGAD sensors", Journal of Synchrotron Radiation, vol. 26, pp. 1226-1237, 2019, DOI: 10.1107/S1600577519005393.